Photoelectron Spectroscopy and Electronic Structures of Fullerene Oxides: $C_{60}O_x^-$ ($x = 1-3$)

Xue-Bin Wang, Hin-Koon Woo, Boggavarapu Kiran, and Lai-Sheng Wang*

Department of Physics, Washington State University, 2710 University Drive, Richland, Washington 99354, and W. R. Wiley Environmental Molecular Sciences Laboratory and Chemical Sciences Division, Pacific Northwest National Laboratory, MS 8-88, P.O. Box 999, Richland, Washington 99352

Received: October 10, 2005; In Final Form: November 1, 2005

We report a photoelectron spectroscopy (PES) study on a series of fullerene oxides, $C_{60}O_x^-$ ($x = 1-3$). The PES spectra reveal one isomer for $C_{60}O^-$, two isomers for $C_{60}O_2^-$, and multiple isomers for $C_{60}O_3^-$. Compared to C_{60}, the electronic structures of $C_{60}O_x$ are only slightly perturbed, resulting in similar anion photoelectron spectra. The electron affinity of $C_{60}O_x$ was observed to increase only marginally with the number of oxygen atoms, x, from 2.683 eV for C_{60}, to 2.745 eV for $C_{60}O$, and 2.785 eV/2.820 eV for $C_{60}O_2$ (two isomers). We also carried out theoretical calculations, which confirmed the observed isomers and showed that all the fullerene oxides are in the form of epoxide. The PES and theoretical calculations, as well as molecular orbital analysis, indicate that addition of oxygen atoms to the C_{60} cage only modifies the local carbon network and leave the rest of the fullerene cage largely intact geometrically and electronically.

Introduction

Fullerene oxides ($C_{60}O_x$), common residues in fullerene bulk synthesis as a result of oxidation, are a class of important functionalized fullerene derivatives. First detected in mass spectrometry and electrochemical oxidation of C_{60},[1,2] the oxides were reported to be the starting materials to form large odd-numbered carbon clusters, such as C_{119}.[3−5] Theoretical calculations suggested that for the fullerene monoxide ($C_{60}O$) there were two isomers, i.e., [6,6]-closed epoxide (**1**) and [5,6]-open oxidoannulene (an ether structure) with comparable stabilities,[6−11] but only the epoxide was initially synthesized[12−14] with the latter missing until more recently.[15] Oxidation of C_{60} with *m*-choroperoxybenzoic acid produced bulk quantities of $C_{60}O_2$ and X-ray diffraction showed it was a fullerene diepoxide with both oxygen atoms positioned over [6,6] ring junctions on a common six-member face of the carbon cage (**2**).[16] HPLC chromatogram analyses of the reaction products of C_{60} with O_3 indicated two isomers for $C_{60}O_2$, one with the proposed structure of **2** and the other one similar to that for **2**, but with the two oxygen atoms bridging the neighboring six-member ring (**3**).[17] The electronic structures and electron affinities (EAs) of $C_{60}O_x$ are expected to play an important role in any of its applications, and extensive electrochemical studies have been pursued as such.[1,18−20] Unlike C_{60} and C_{60}^-, which have been intensively investigated using gas phase photoelectron spectroscopy (PES) since the early stage of its discovery[21−24] and recently revisited with vibrational resolution,[25−27] no gas-phase PES study is available for $C_{60}O_x$ and their anions.

In this Letter, we report the first PES study of $C_{60}O_x^-$ in the gas phase. The PES spectra were taken at 70 K with three different photon energies using a recently constructed low-temperature electrospray PES apparatus. Our PES spectra show that all oxides have electronic structures similar to that for C_{60}, with only a slight increase of EA as the number of oxygen atoms increases. We observe one isomer for $C_{60}O$, two isomers for $C_{60}O_2$, and multiple isomers for $C_{60}O_3$. Theoretical calculations were carried out to provide further insight into the electronic and structural properties of the fullerene oxides.

Experimental Details

The experiments were carried out using a newly developed low-temperature PES apparatus, which consists of an electro-spray ionization source (ESI), a cryogenically cooled ion trap time-of-flight mass spectrometry, and a magnetic bottle time-of-flight photoelectron analyzer.[27] The ESI source and the magnetic-bottle photoelectron spectrometer are similar to that described previously.[28] $C_{60}O_x^-$ anions were produced as byproducts from a solution intended to generate C_{60}^- anions in an acetonitrile solution.[29] After guided by a RF-only octopole and a quadrupole mass filter (operated in the RF-only mode), all anions were turned 90° via a quadruple ion bender and entered into a three-dimensional Paul trap for ion accumulation and collision cooling. The ion trap was attached to a cold head of a cryostat and its temperature can be controlled from 10 to 400 K. For the current experiment, the trap was kept at 70 K and the collision background gas used was 10^{-4} Torr N_2. The cooled ions were pulsed out of the trap at a 10 Hz repetition rate and separated in a linear TOF mass spectrometer according to their respective mass-to-charge ratios. The $C_{60}O_x^-$ ($x = 0-3$) anions of interest were selected by a pulsed mass-gate, and decelerated before being intercepted by a detachment laser beam in the interaction zone of the magnetic-bottle electron analyzer. In the current experiment, three detachment photon energies were used: 355 nm (3.496 eV) and 266 nm (4.661 eV) from a Nd: YAG laser, and 193 nm (6.424 eV) from an excimer laser. The detachment laser was operated at 20 Hz with the ion beam off

---

* Corresponding author. E-mail: ls.wang@pnl.gov.

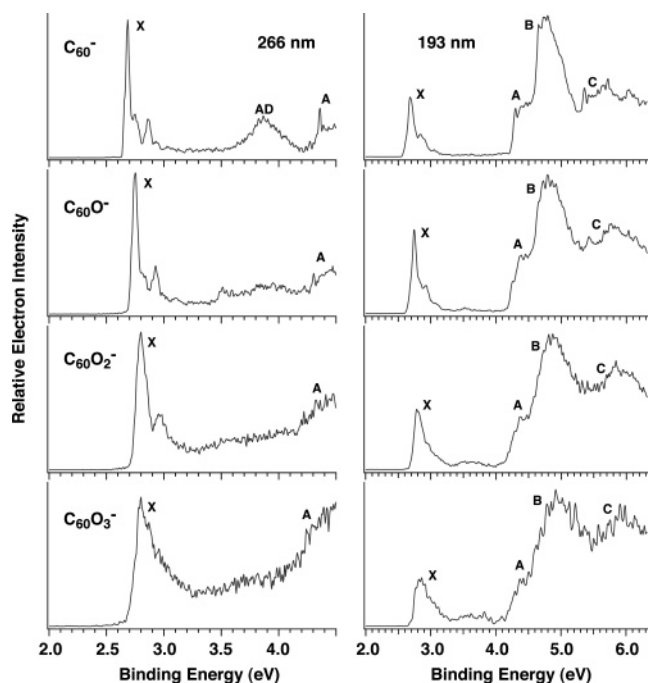**11090** *J. Phys. Chem. A, Vol. 109, No. 49, 2005*

Letters

Figure 1. Photoelectron spectra of $C_{60}O_x^-$ ($x = 1-3$) at 266 nm (4.661 eV) and 193 nm (6.424 eV), compared with that of C_{60}^- from ref 27.

on alternate shots for background subtraction. The photodetached electrons were collected with nearly 100% efficiency by the magnetic-bottle and analyzed in a 5.2 m long electron flight tube. The electron energy resolution of the apparatus is $\Delta E/E \sim 2\%$, i.e., 20 meV for 1 eV electrons. Photoelectron time-of-flight spectra were collected and then converted to kinetic energy spectra, calibrated by the known spectra of I^- and ClO_2^-.[30] The electron binding energy spectra presented here were obtained by subtracting the kinetic energy spectra from the detachment photon energies.

Theoretical Methods

All calculations were done at the level of generalized gradient approach using the Perdew–Wang exchange-correlation functional.[31] The standard Slater-type-orbital (STO) basis set with quality of triple-ζ plus with two sets of polarization functions (TZ2P) were used for the valence orbitals of all the atoms, with frozen core approximation. The geometries of all molecules (both anions and neutrals) were fully optimized with default convergence criteria. The adiabatic detachment energies (ADEs) were obtained by taking the energy difference between the anions and the neutrals in their optimized geometries. All the calculations were accomplished using the Amsterdam density functional (ADF 2004.01) program.[32]

Experimental Results

Figure 1 shows the PES spectra of $C_{60}O_x^-$ ($x = 1-3$) at 266 nm (left) and 193 nm (right). The low-temperature spectra of

C_{60}^-, which have been recently reported,[27] are shown for comparison. Major spectral features are labeled X, A, B, and C in the order of increasing electron binding energies. Surprisingly, the spectra of the $C_{60}O_x^-$ oxides are very similar to that of C_{60}^-. In particular, the spectra of $C_{60}O^-$ are almost identical to those of C_{60}^- with only a slight increase of electron binding energies. The HOMO–LUMO gap of $C_{60}O$, defined by the X–A separation, is 1.52 eV, which is only slightly lower than that of C_{60} (1.62 eV).[27] The quality of the spectra for $C_{60}O_2^-$ and $C_{60}O_3^-$ was poorer due to their weak mass intensities, but their similarity to the C_{60}^- spectra is obvious. Even the autodetachment features, labeled "AD" in the 266 nm spectrum of C_{60}^-, are also present in the oxide spectra as weak signals in the HOMO–LUMO band gap region. Vibrational structures were also discernible in the X band of the oxide spectra at both 193 and 266 nm, and they also appeared to be similar to that of the C_{60}^- spectra. The HOMO–LUMO gaps of $C_{60}O_2$ and $C_{60}O_3$ are estimated to be 1.5 eV, similar to that of $C_{60}O$. Due to existence of multiple isomers for the higher oxides (as discussed below) and poorer resolution, the 1.5 eV HOMO–LUMO gap should be regarded as the average of the different isomers. The HOMO–LUMO gaps for all species are summarized in Table 1.

The details of the vibrational structures in the first PES band of $C_{60}O_x^-$, were revealed more clearly at 355 nm (Figure 2). Vibrational structures of $C_{60}O^-$ are seen to be identical to that of C_{60}^-, even though the resolution of the $C_{60}O^-$ spectrum was slightly poorer. This observation suggests that the vibrational modes and their frequencies excited in the ground-state transition in $C_{60}O^-$ and C_{60}^- are identical; i.e., the O atom has very little perturbation to the electronic and geometrical structures of the C_{60} cage in $C_{60}O$, indicating the electronic and structural robustness of the C_{60} cage structure. The EA of $C_{60}O$ is measured accordingly from the 0–0 transition to be 2.745 eV, compared to 2.683 eV for C_{60} in Table 1.

The vibrational structures in the 355 nm spectrum of $C_{60}O_2^-$ were poorly resolved. However, two peaks (X_1 and X_2) were resolved for what appeared to be the 0–0 transition. These two peaks could be due to a vibrational progression of a low frequency mode. But they are most likely due to the 0–0 transitions for two isomers of $C_{60}O_2^-$, as verified below by the theoretical calculations. From the peak positions of X_1 and X_2, we obtained the ADEs for these two isomers of $C_{60}O_2^-$ as 2.785 eV (X_2) and 2.820 eV (X_1). The 355 nm spectrum of $C_{60}O_3^-$ was even less resolved, partly due to the poorer resolution and partly due to the fact that multiple isomers were expected to be present for $C_{60}O_3^-$. Thus, we could not obtain the ADE for $C_{60}O_3^-$. An estimate of 2.8 eV is listed in Table 1, which should be viewed as an average of the different isomers.

Theoretical Results

We carried out theoretical calculations using density functional theory with the TZ2P basis set. For $C_{60}O^-$, the lowest

TABLE 1: Experimental and Theoretical Adiabatic Detachment Energies (ADEs) of C_{60}^- and $C_{60}O_x^-$ ($x = 1-3$) and the Measured HOMO–LUMO Gaps for the Neutral Species (All Energies in eV)

	C_{60}^-	$C_{60}O^-$	$C_{60}O_2^-$ (isomer 1)	$C_{60}O_2^-$ (isomer 2)	$C_{60}O_3^-$
ADE (expt)[a,b]	2.683(8)	2.745(8)	2.820(10)	2.785(10)	~2.8
ADE (cal)	2.86	2.95	3.02	3.00	
HOMO–LUMO gap	1.62 ± 0.01[c]	1.52 ± 0.01	~1.5	~1.5	~1.5

[a] The ADEs were determined from the 0–0 transitions in the 355 nm spectra (Figure 2) except for $C_{60}O_3^-$, for which only a rough estimate from the detachment threshold was obtained. The ADEs also represent the EA of the corresponding neutral species. [b] Numbers in parentheses are uncertainties in the last digits. [c] From ref 27.
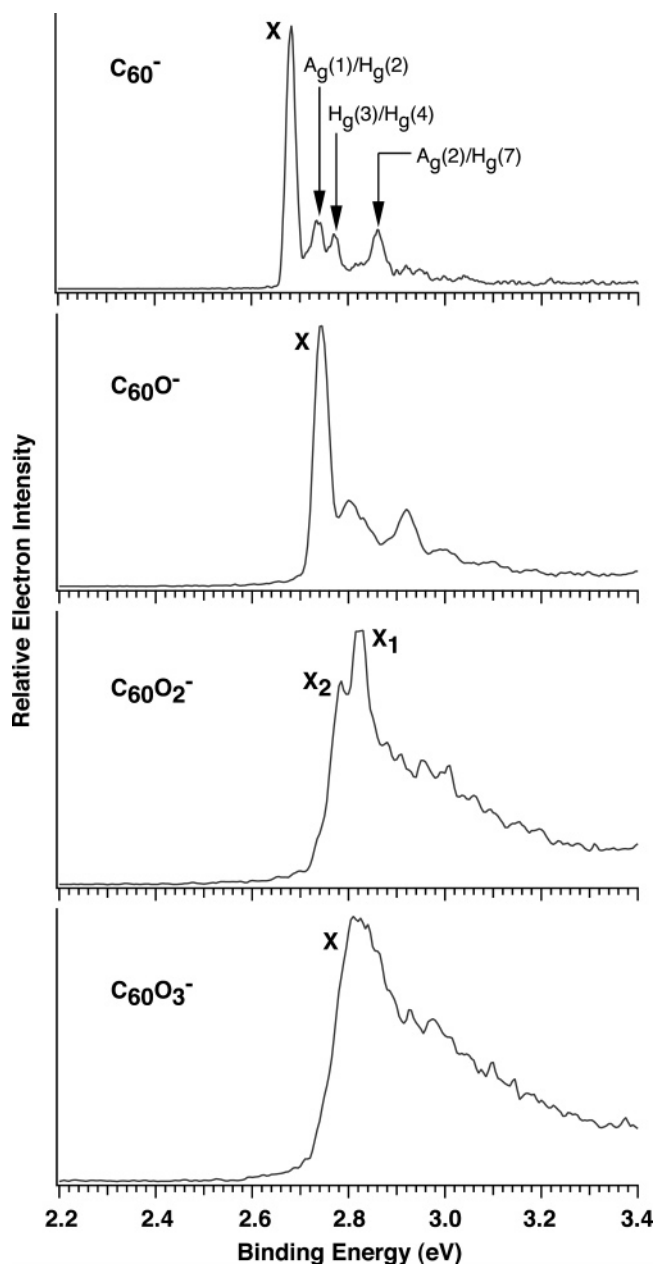
Figure 2. Photoelectron spectra of $C_{60}O_x^-$ ($x = 1-3$) at 355 nm (3.496 eV), compared with that of C_{60}^- from ref 27 with assignments of the main vibrational features.
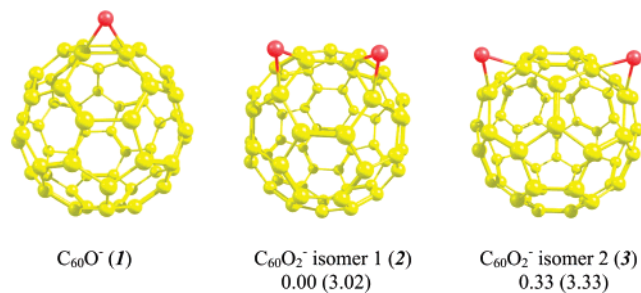

$C_{60}O^-$ (**1**) $C_{60}O_2^-$ isomer 1 (**2**) $C_{60}O_2^-$ isomer 2 (**3**)
0.00 (3.02)   0.33 (3.33)

Figure 3. Optimized structures of $C_{60}O^-$ (**1**) and $C_{60}O_2^-$ (**2, 3**). The numbers are the relative energies in electronvolts for the anions and the neutrals (in parentheses).

energy structure is the epoxide structure with the oxygen bridging one [6,6] C−C bond (**1**) (Figure 3). We identified two low-lying diepoxide isomers for $C_{60}O_2^-$ separated by only 0.33 eV in energy. For the more stable isomer 1 (**2**), the two oxygen atoms position over [6,6] ring junctions on one six-member ring,
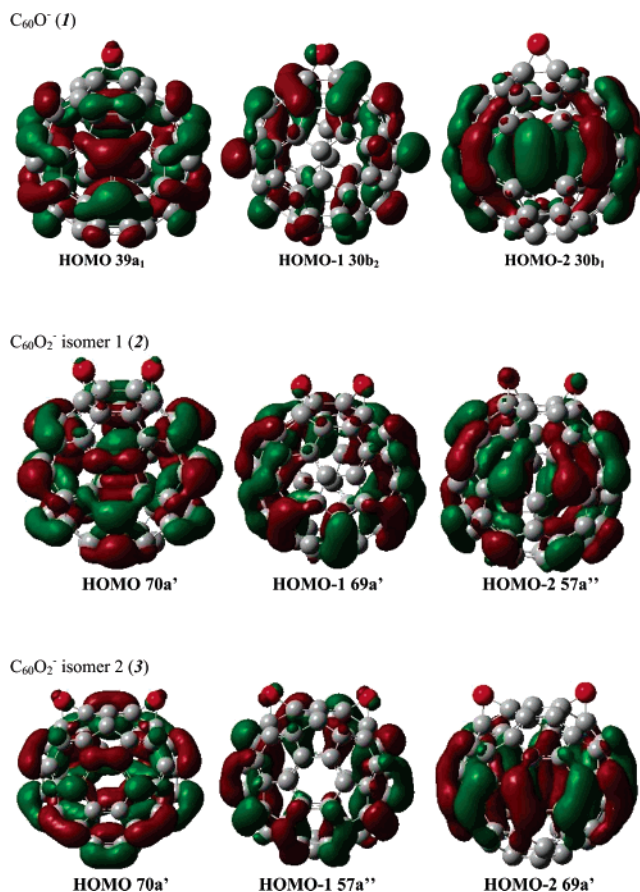

Figure 4. First three highest occupied molecular orbitals of $C_{60}O^-$ (**1**) and $C_{60}O_2^-$ (**2, 3**).

whereas for isomer 2 (**3**) they bridge the [6,6] C−C bond over neighboring six-member rings (Figure 3). The energetics of $C_{60}O_2$ neutrals are similar to that of the anions, and isomer 2 is 0.31 eV higher in energy. The calculated ADEs for $C_{60}O^-$ and $C_{60}O_2^-$ are compared with the experimental values in Table 1. The calculated values are ~0.2 eV higher than the experimental ones but reproduce the experimental trend well. Particularly, the calculation predicts that the more stable isomer 1 of $C_{60}O_2^-$ has a slightly higher ADE compared to that of isomer 2, consistent with the experimental observation (Figure 2).

Discussions

The PES spectra of C_{60}^- have been reported before and are well understood.[25−27] The HOMO of C_{60} is a 5-fold degenerate h_u orbital. In C_{60}^-, the extra electron enters the LUMO of C_{60}, t_{1u}, which is subject to Jahn−Teller distortion, giving rise to a complicated vibrational structure for the transition from the ground state of C_{60}^- ($^2T_{1u}$) to the ground state of C_{60} neutral (^1A_g) because of the vibronic coupling with the two A_g and eight H_g modes. This has been discussed in detail before[25−27] and several assignments are reproduced in Figure 2 for C_{60}^-. The apparent similarity between the $C_{60}O_x^-$ and C_{60}^- spectra indicates the oxides have electronic and geometrical structures essentially similar to that of C_{60} although the overall symmetries are lower for the oxides. This is born out from the calculations. As shown in Figure 3, each oxygen atom breaks one C=C double bond to form two epoxide bonds locally and does not seem to induce global changes to the cage. The valence MOs of the oxides are still expected to be composed of the p orbitals from the cage (C−C π orbital), very much like the bare C_{60}. These are shown clearly in Figure 4. We note that the O atoms

have very little contribution to the valence MOs of the oxides and they only affect the proximal carbons. Thus the $C_{60}O_x$ oxides can be viewed as O atoms chemisorbed to the C_{60} surface.

According to geometrical structure analyses, there can be two isomers for the fullerene monoxide $C_{60}O$ ([5,6]-open oxidoannulene and [6,6]-closed epoxide) and eight isomers for the fullerene dioxide $C_{60}O_2$.[10] Although the two isomers of $C_{60}O$ are predicted to have similar stabilities with a high conversion barrier between them, experimentally only the epoxide was found initially.[12-14] The [5,6]-open isomer has been discovered more recently with photolysis of a C_{60} ozonation solution.[15] We believe the monoxide observed in our experiment is the [6,6]-closed epoxide because it was produced via slow thermal reaction of C_{60} with O_2, as reported similarly in the literature.[1,12-14] For $C_{60}O_2$, we observed two dominant isomers (**2**, **3**) among eight possible ones, also consistent with the previous studies.[16,17] The broadness of our PES spectra of $C_{60}O_3^-$ indicates the presence of multiple isomers. This observation agrees with two previous reports showing three isomers existed for the trioxides in the product mixtures of oxidation of fullerenes by ozone.[33,34]

In conclusion, we report a combined PES and theoretical study on a series of fullerene oxides, $C_{60}O_x$ ($x = 1-3$). Our spectra reveal similar electronic structures for the oxides compared to that of C_{60}. This similarity is confirmed via MO analyses. The EAs of $C_{60}O_x$ are found to increase slightly with the oxygen content, x. We observed one isomer for $C_{60}O^-$, two dominant isomers for $C_{60}O_2^-$, and multiple isomers for $C_{60}O_3^-$. Our results showed that O atoms only perturb the C_{60} cage locally and have very little global effect on the C_{60} cage. This finding demonstrates the electronic and structural stability of the C_{60} cage.

References and Notes

(1) Kalsbeck, W. A.; Thorp, H. H. *J. Electroanal. Chem.* **1991**, *314*, 363.

(2) Wood, J. M.; Kahr, B.; Hoke, S. H., II; Dejarme, L.; Cooks, R. G.; Ben-Amotz, D. *J. Am. Chem. Soc.* **1991**, *113*, 5907.

(3) McElvany, S. W.; Callahan, J. H.; Ross, M. M.; Lamb, L. D.; Huffman, D. R. *Science* **1993**, *260*, 1632.

(4) Deng, J.-P.; Ju, D.-D.; Her, G.-R.; Mou, C.-Y.; Chen, C.-J.; Lin, Y.-Y.; Han, C.-C. *J. Phys. Chem.* **1993**, *97*, 11575.

(5) Beck, R. D.; Brauchle, G.; Stoermer, C.; Kappes, M. *J. Chem. Phys.* **1995**, *102*, 540.

(6) Raghavachari, K. *Chem. Phys. Lett.* **1992**, *195*, 221.

(7) Raghavachari, K.; Sosa, C. *Chem. Phys. Lett.* **1993**, *209*, 223.

(8) Menon, M.; Subbaswamy, K. R. *Chem. Phys. Lett.* **1993**, *201*, 321.

(9) Wang, B.-C.; Chen, L.; Chou, Y.-M. *J. Mol. Struct.* **1998**, *422*, 153.

(10) Wang, B.-C.; Chen, L.; Lee K.-J.; Cheng, C.-Y. *J. Mol. Struct.* **1999**, *469*, 127.

(11) Manoharan, M. *J. Org. Chem.* **2000**, *65*, 1093.

(12) Creegan, K. M.; Robbins, J. L.; Robins, W. K.; Millar, J. M.; Sherwood, R. D.; Tindall, P. J.; Cox, D. M. *J. Am. Chem. Soc.* **1992**, *114*, 1103.

(13) Elemes, Y.; Silverman, S. K.; Sheu, C.; Kao, M.; Foote, C. S.; Alvarez, M. M.; Whetten, R. L. *Angew. Chem., Int. Ed. Engl.* **1992**, *31*, 351.

(14) Balch, A. L.; Costa, D. A.; Lee, J. W.; Noll, B. C.; Olmstead, M. M. *Inorg. Chem.* **1994**, *33*, 2071.

(15) Weisman, R. B.; Heymann, D.; Bachino, S. M. *J. Am. Chem. Soc.* **2001**, *123*, 9720. Tsyboulski, D.; Heymann D.; Bachino, S. M.; Alemany L. B.; Weisman, R. B. *J. Am. Chem. Soc.* **2004**, *126*, 7350.

(16) Balch, A. L.; Costa, D. A.; Noll, B. C.; Olmstead, M. M. *J. Am. Chem. Soc.* **1995**, *117*, 8926.

(17) Deng, J.-P.; Mou, C.-Y.; Han, C.-C. *J. Phys. Chem.* **1995**, *99*, 14907.

(18) Fedurco, M.; Costa, D. A.; Balch, A. L.; Fawcett, W. R. *Angew. Chem., Int. Ed. Engl.* **1995**, *34*, 194.

(19) Winkler, K.; Costa, D. A.; Balch, A. L.; Fawcett, W. R. *J. Phys. Chem.* **1995**, *99*, 17431.

(20) Echegoyen, L.; Echegoyen, L. E. *Acc. Chem. Res.* **1998**, *31*, 593.

(21) Yang, S. H.; Pettiette, C. L.; Conceicao, J.; Cheshnovsky, O.; Smalley, R. E. *Chem. Phys. Lett.* **1987**, *139*, 233.

(22) Wang, L. S.; Conceicao, J.; Jin, C.; Smalley, R. E. *Chem. Phys. Lett.* **1991**, *182*, 5.

(23) Wang, L. S.; Alford, J. M.; Chai, Y.; Diener, M.; Zhang, J.; McClure, S. M.; Guo, T.; Scuseria, G. E.; Smalley, R. E. *Chem. Phys. Lett.* **1993**, *207*, 354.

(24) Brink, C.; Anderson, L. H.; Hvelplund, P.; Mathur, D.; Voldstad, J. D. *Chem. Phys. Lett.* **1995**, *233*, 52.

(25) Gunnarsson, O.; Handschuh, H.; Bechthold, P. S.; Kessler, B.; Ganteför, G.; W. Eberhardt, W. *Phys. Rev. Lett.* **1995**, *74*, 1875.

(26) Wang, X. B.; Ding, C. F.; Wang, L. S. *J. Chem. Phys.* **1999**, *110*, 8217.

(27) Wang, X. B.; Woo, H. K.; Wang, L. S. *J. Chem. Phys.* **2005**, *123*, 051106−1−4.

(28) Wang, L. S.; Ding, C. F.; Wang, X. B.; Barlow, S. E. *Rev. Sci. Instrum.* **1999**, *70*, 1957.

(29) Subramanian, R.; Boulas, P.; Vijayashree, M. N.; D'Souza, F.; Jones, M. T.; Kadish, K. M. *J. Chem. Soc. Chem. Commun.* **1994**, 1847.

(30) Gilles, M. K.; Polak, M. L.; Lineberger, W. C. *J. Chem. Phys.* **1992**, *96*, 8012.

(31) (a) Perdew, J. P.; Wang, Y. *Phys. Rev. B* **1992**, *45*, 13244, (b) Perdew, J. P.; Chevary, J. A.; Vosko, S. H.; Jackson, K. A.; Perderson, M. R.; Singh, D. J.; Foilhais, C. *Phys. Rev. B* **1992**, *46*, 6671.

(32) ADF. 2004.01 SCM, Theoretical Chemistry, Vrije Universiteit, Amsterdam, The Netherlands.

(33) Deng, J. P.; Mou, C. Y.; Han, C. C. *Fullerene Sci. Technol.* **1997**, *5*, 1033.

(34) Deng, J. P.; Mou, C. Y.; Han, C. C. *Fullerene Sci. Technol.* **1997**, *5*, 1325.